



Original Research Article

Synthesis and Characterization of Zinc Sulfide Nanostructure by Sol Gel Method

Alaa Abd Al-Zahra* , Abdul Karim M. A. Al-Sammarraie

University of Baghdad, College of Science, Department of Chemistry, Baghdad, Iraq

ARTICLE INFO

Article history

Submitted: 2021-10-20

Revised: 2021-10-24

Accepted: 2021-10-30

Manuscript ID: CHEMM-2110-1388

Checked for Plagiarism: **Yes**

Language Editor:

[Dr. Behrouz Jamalvandi](#)

Editor who approved publication:

[Dr. Mohsen Oftadeh](#)

DOI: 10.22034/chemm.2022.1.7

KEYWORDS

Sol-gel processing

UV-visible spectroscopy

Fourier Transform Infrared (FTIR)

Spectroscopy

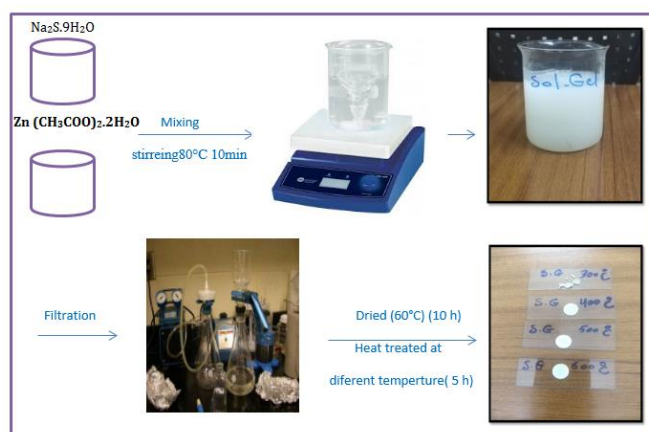
Scanning electron microscopy (SEM)

X-ray diffraction (XRD)

ABSTRACT

At four different temperatures, a sol-gel technique was used to create ZnS semiconductor nanoparticles using zinc acetate and Sodium sulphid as source materials of Zn and S, respectively. Scanning electron microscopy (SEM) was used to determine the particle size and surface morphology of the produced ZnS nanoparticles, showing a spherical ZnS particle with a diameter of about 24 nm. The cubic crystal structure of ZnS was found by X-ray diffraction (XRD). The zinc-sulfur band can be seen at 420 cm^{-1} in spectroscopy. The visible and ultraviolet absorption spectra of ZnS NP revealed a blue shift at a maximum of 315 nm.

GRAPHICAL ABSTRACT



* Corresponding author: Alaa Abd Al-Zahra

✉ E-mail: thechimalaa@gmail.com

© 2022 by SPC (Sami Publishing Company)

Introduction

Semiconductor nanostructure materials have become highly prominent in recent years as a result of quantum confinement phenomena due to their unique optical and electrical capabilities [1-3]. As one of the most important II-IV semiconductors, ZnS offers a wide range of applications, like, Light Emitting Diode (LED) [4], phosphors [5,6], nonlinear optical devices [7] pharmaceuticals [8,9], electroluminescence [10] and fluorescence probe [11].

The temperature of the synthesis plays a significant effect in particle shape and size management [12]. The kinetics and thermodynamics of the process have an impact on particle growth. Temperature can influence the particle growth mechanism, i.e., the Ostwald ripening process, via interfacial energy, diffusion and growth rate parameters, and equilibrium solubility [13]. However, the method of synthesis has a considerable impact on its properties. Synthesizing ZnS thin films has been done using a variety of techniques, including: chemical spray pyrolysis [14,15], solvothermal synthesis [16,17], successive ionic layer adsorption and reaction [18,19], pulsed laser deposition [20], metal-organic chemical vapor deposition [21], RF-magnetron sputtering [22,23], electro deposition [24,25], thermal evaporation [26], electron beam evaporation [27], aerosol assisted chemical vapour deposition [28, 29] and chemical bath deposition [30,31].

Materials and methods

All of the reagents, including zinc acetate and sodium sulphid, were acquired from Sigma-Aldrich and were used without additional purification. As a solvent, we utilized de-ionized water. Zinc acetate $Zn(CH_3COO)_2 \cdot 2H_2O$ (2.194 g), and $Na_2S \cdot 9H_2O$ (4.8038 g) were dissolved in deionized water and stirred at ambient temperature for 15 min. Then, they were stirred together and heated on a magnetic stirrer to 80°C, stirring at a set speed. The gel is created after 10 minutes. To eliminate superfluous water, this viscous gel was dried in a heating oven at 60 °C for 10 hours. The dried powder was then

heated for 5 hours at 300 °C, 400 °C, 500 °C, and 600 °C, respectively to obtain the final product.

X-ray diffraction was used to examine the structure of the ZnS samples, with a Siemens model D500, SEM ZEISS model: sigma VPEDS, and mapping by Oxford Instruments, UK. The Fourier transform infrared spectroscopy (FTIR) Shimadzu FT-IR8400S Japan chemistry department, college of science, Baghdad university, was used to examine the composition and quality of the substance in the range (4000-400 cm^{-1}). Shimadzu UV 1800 twin beam, Japan, area (200-1100) nm, was used to get the absorption spectra.

Morphological observation

Figure 1 illustrates the SEM pictures of each synthesized sample. SEM micrographs of produced ZnS nanoparticles with spherical shaped are shown in Figures 1(a, b, c, and d). The size of the crystals grows as the temperature of growth rises. Crystals of modest size are visible in the sample developed at 300°C. Particles agglomerate and plate-shaped big clusters form when the temperature of the growing medium rises.

Structural studies

Figure 2 shows the X-Ray diffraction patterns of Zinc Sulfide nanoparticles synthesized at different temperatures (300, 400, 500 and 600 °C). All samples had peaks on their XRD patterns, indicating they formed a cubic structure, which was further validated by mapping with JCPDS No: 05-0566. The diffraction peaks are located in the planes (111), (200), (220), (311), (400), (331), and (422). 32.05, 34.69, 36.42, 47.75, 56.81, 63.13, and 68.24 correspond to the two θ at 32.05, 34.69, 36.42, 47.75, 56.81, 63.13, and 68.24.

Table 1 shows the computed lattice parameters. The Wulf - Bragg relation is used to compute the distances d_{hkl} between successive lattice planes:

$$2d_{hkl} \sin \theta = n \lambda \quad 1$$

The Debye - Scherrer equation was used to compute the powder's average crystalline size. [32-34]:

$$D = 0.9 \lambda / \beta \cos \theta \dots \quad 2$$

D is the mean crystallite size, λ is the wavelength of X-ray (0.15418 nm), θ is degree of the diffraction peak/the Bragg's angle, and β is the full width at half maximum of the XRD peak appearing at the diffraction angle θ . The average

crystallite sizes of ZnS (NPS) are found to be 15nm, 24nm, 17nm and 21nm for samples 300,400,500and6000c, respectively.

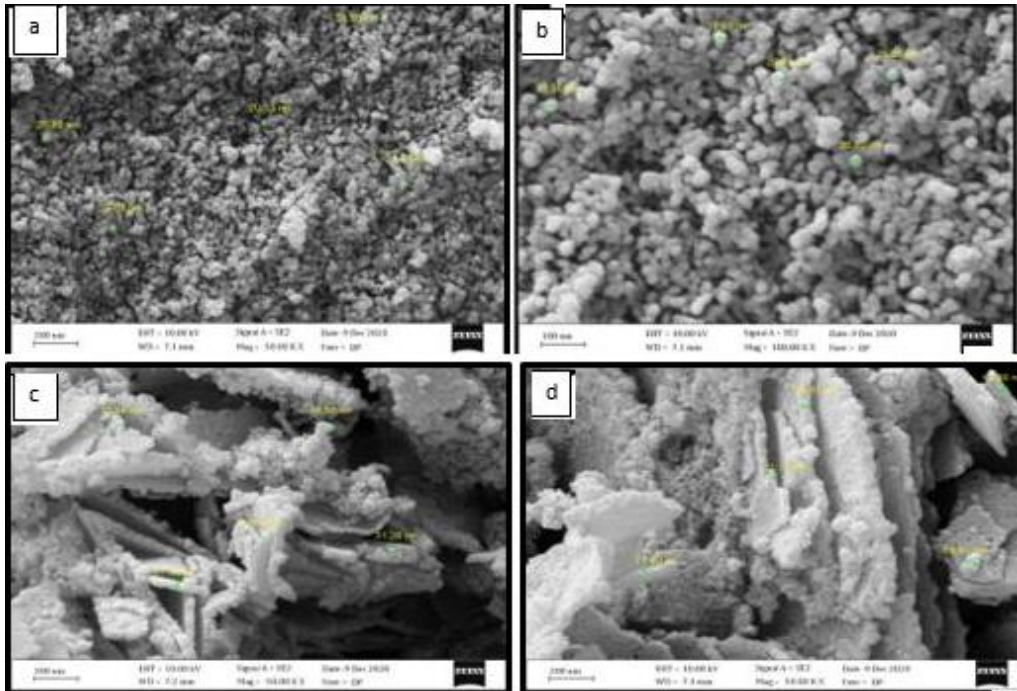


Figure 1: SEM images of synthesized ZnS (a, b, c, d) sample

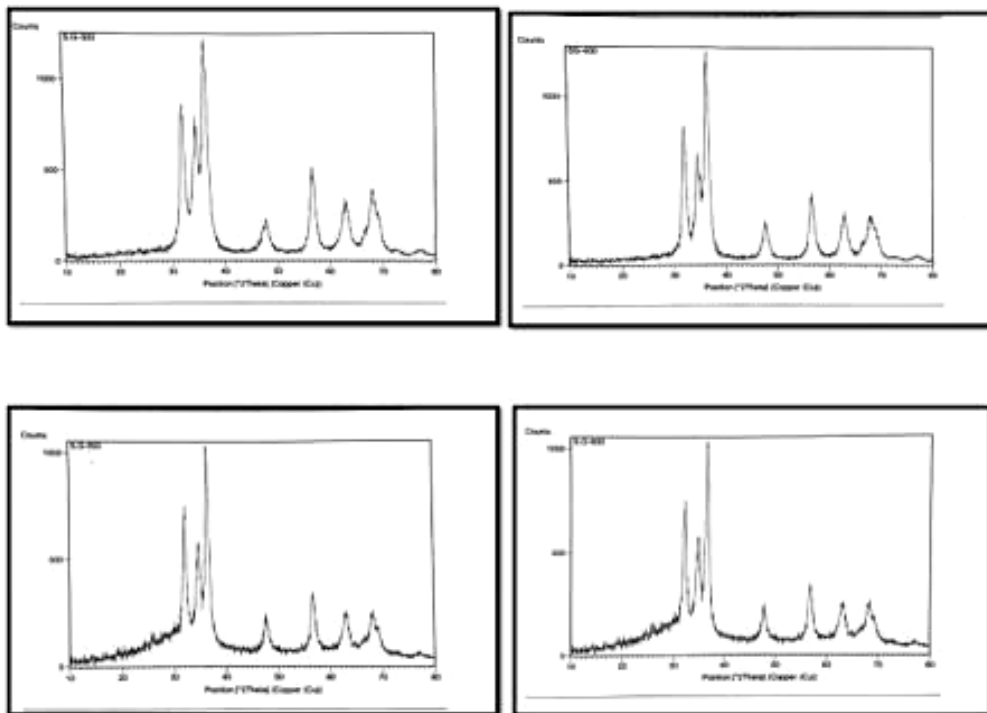


Figure 2: XRD plots of ZnS nanoparticles at 300 °C, 400 °C, 5000C and 600 °C

Table 1: Nano crystal sizes and Lattice constants calculated from XRD ($\lambda=0.154\text{nm}$) patterns for samples a, b, c and sample d

sample	plane	2θ (degree)	(Interplanar distance) $d = \lambda/2\sin\theta$	FWHM (β) (degree)	D (nm)
300 °C	111	32.1814	0.2778	0.2952	15
	200	34.6037	0.2589	0.7872	
	220	36.4404	0.2463	0.2952	
	311	47.8228	0.1899	1.1808	
	400	56.8249	0.1618	0.8856	
	331	63.0462	0.1473	1.18087	
	422	68.1466	0.1374	0.7872	
400 °C	111	31.9725	0.2796	0.2460	24
	200	34.6165	0.2589	0.2952	
	220	36.4367	0.2464	0.2460	
	311	47.6914	0.1905	0.6888	
	400	56.7296	0.1621	0.8856	
	331	63.0520	0.1473	1.1808	
	422	68.0980	0.1374	0.4920	
500 °C	111	32.0745	0.2788	0.4428	17
	200	34.7295	0.2581	0.6888	
	220	36.5318	0.2460	0.2952	
	311	47.8532	0.1899	0.7872	
	400	56.8724	0.1617	0.7873	
	331	63.1386	0.1471	0.8856	
	422	68.1335	0.1375	0.3936	
600 °C	111	32.0547	0.2789	0.1968	21
	200	34.6995	0.2583	0.6888	
	220	36.4259	0.2464	0.2460	
	311	47.7532	0.1903	0.6888	
	400	56.8161	0.1619	0.6888	
	331	63.1397	0.1471	0.8856	
	422	68.2466	0.1372	0.6888	

Composition studies

Figure 3 shows the FT-IR spectra of ZnS nanoparticles. Sol gel technique was used to prepare this sample, ranging $4000 - 400\text{cm}^{-1}$. FT-IR measurements were performed when it is at room temperature.

The vibration of ZnS nanoparticles is associated with the bands between 420 and 1100cm^{-1} . The

presence of residues of organic species (e.g. COO) on the particle surface is linked to the coordination of carboxyl groups, resulting in the distinctive absorption bands at 1631cm^{-1} . The band at 2920cm^{-1} is used to deduce the C-H stretching vibration. At 3450cm^{-1} , the broad band corresponds to -OH stretching absorbed on the surface of the H_2O molecule [35,36].

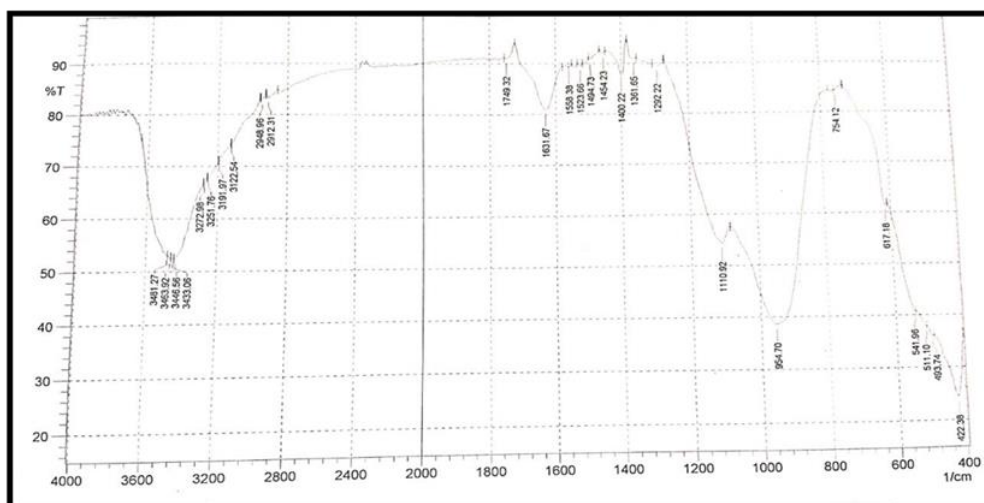


Figure 3: FT-IR spectra of annealed ZnS nanoparticles at (3000C, 4000C, 5000C and 600 °C)

UV-Visible study

The ZnS samples' spectra are shown in Figure 4. It shows a strong absorption peak by ZnS around

400 nm corresponding to the optical band gap [37,38].

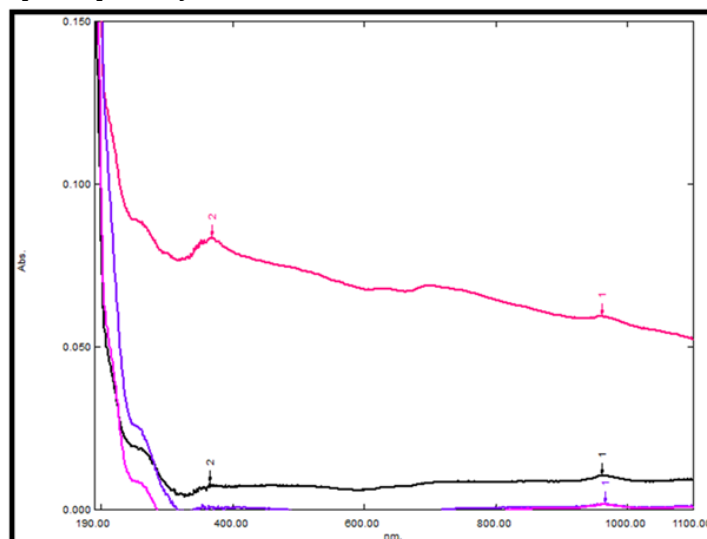


Figure 4: Absorption spectra for ZnS nanostructures prepared at different temperature

Conclusion

A sol gel technique was used to successfully produce Nano crystalline ZnS at (300, 400, 500 and 600 °C). UV-Visible spectra revealed that there was a blue shift in the absorption band at max 315nm. In XRD spectra, the particle size (15-24nm) was calculated by the Debye Scherrer formula; the synthesized particles had a cubic structure of zinc mixture.

Acknowledgments

I would like to thank all member staff of department of Chemistry, University of Baghdad.

Funding

This research did not receive any specific grant from funding agencies in the public, commercial, or not-for-profit sectors.

Authors' contributions

All authors contributed toward data analysis, drafting and revising the paper and agreed to be responsible for all the aspects of this work.

Conflict of Interest

We have no conflicts of interest to disclose.

ORCID

Alaa Abd AL-Zahra:

<https://orcid.org/0000-0002-6583-5063>

References

- [1]. Lee G.J., Chen H.C., Wu J.J., *Int. J. Hydrog. Energy*, 2018, **44**:110117 [[Crossref](#)], [[Google Scholar](#)], [[Publisher](#)]
- [2]. D'Amico P., Calzolari A., Ruini A., Catellani A., *Sci. Rep.*, 2017, **7**:1 [[Crossref](#)], [[Google Scholar](#)], [[Publisher](#)]
- [3]. Rodríguez G.S., Torres R.C.C., Zeferino R.S., Ramos M.E.Á., *Opt. Mater.*, 2019, **89**:396 [[Crossref](#)], [[Google Scholar](#)], [[Publisher](#)]
- [4]. Tran M.T., Hung N.D., Van Q.N., Huyen N.T., Tu N., Thanh H.P., *Opt. Mater.*, 2021, **121**:111587 [[Crossref](#)], [[Google Scholar](#)], [[Publisher](#)]
- [5]. Vijayan S., Dash C.S., Umadevi G., Sundararajan M., Mariappan R., *J. Clust. Sci.*, 2020, 1-8 [[Crossref](#)], [[Google Scholar](#)], [[Publisher](#)]
- [6]. Karthikeyan B., Arun A., Harini L., Sundar K., Kathiresan T., *Biol. Trace. Element. Res.*, 2016, **170**:390 [[Crossref](#)], [[Google Scholar](#)], [[Publisher](#)]
- [7]. Kumar P., Maikap S., Singh K., Chatterjee S., Chen Y.Y., Cheng H.M., Mahapatra R., Qiu J.T., Yang J.R., *J. Electrochem. Soc.*, 2016, **163**:B580 [[Crossref](#)], [[Google Scholar](#)], [[Publisher](#)]
- [8]. Fu L., Fu Z., *Cera. Int.*, 2015, **41**:2492 [[Crossref](#)], [[Google Scholar](#)], [[Publisher](#)]
- [9]. Dash C.S., Sahoo S., Prabakaran, S.R.S., *Solid State Ion.*, 2018, **324**:218225 [[Crossref](#)], [[Google Scholar](#)], [[Publisher](#)]
- [10]. Dash C.S., Prabakaran S.R.S., *Adv. Mater. Sci.*, 2019, **58**:248270 [[Crossref](#)], [[Google Scholar](#)], [[Publisher](#)]
- [11]. Azizi S., Ahmad M.B., Namvar F., Mohamad R., *Mater. Lett.*, 2014, **116**:275 [[Crossref](#)], [[Google Scholar](#)], [[Publisher](#)]
- [12]. Mott D., Galkowski J., Wang L., Luo, J., Zhong C.J., *Langmuir*, 2007, **23**:5740 [[Crossref](#)], [[Google Scholar](#)], [[Publisher](#)]
- [13]. Madras G., McCoy B.J., *J. Chem. Phys.*, 2003, **119**:1683 [[Crossref](#)], [[Google Scholar](#)], [[Publisher](#)]
- [14]. Safeera, T.A., Anju K.J., Joffy P.J., Anila E.I., *Solid State Phys.*, 2013, **1512**:668 [[Crossref](#)], [[Google Scholar](#)], [[Publisher](#)]
- [15]. Zeng, X., et al., *Chem. Phys.*, 2013, **15**:6763 [[Crossref](#)], [[Google Scholar](#)], [[Publisher](#)]
- [16]. Akhtar M.S., Riaz S., Mehmood R.F., Ahmad K.S., Alghamdi Y., Malik M.A., Naseem S., *Mater. Chem. Phys.*, 2017, **189**:28 [[Crossref](#)], [[Google Scholar](#)], [[Publisher](#)]
- [17]. Zhang Y., Mi L., *Chem. Lett.*, 2012, **41**:915 [[Crossref](#)], [[Google Scholar](#)], [[Publisher](#)]
- [18]. Turgut, G., Keskenler E.F., Aydın S., Doğan S., Duman S., Sönmez E., Esen B., Düzgün B., *Mater. Lett.*, 2013, **102-103**:106 [[Crossref](#)], [[Google Scholar](#)], [[Publisher](#)]
- [19]. Fischereder A., Martinez-Ricci M.L., Wolosiuk A., Haas W., Hofer F., Trimmel G., Soler-Illia G.J., *Chem. Mater.*, 2012, **24**:1837 [[Crossref](#)], [[Google Scholar](#)], [[Publisher](#)]
- [20]. Zhang W., Zeng X., Lu J., Chen H., *Mater. Res. Bull.*, 2013, **48**:3843 [[Crossref](#)], [[Google Scholar](#)], [[Publisher](#)]
- [21]. Yoon Y.G., Choi I.H., *J. Korean Phys. Soc.*, 2013, **63**:1609 [[Crossref](#)], [[Google Scholar](#)], [[Publisher](#)]
- [22]. Yoo D., Choi M.S., Heo S.C., Chung C., Kim D., Choi C., *Met. Mater. Int.*, 2013, **19**:1309 [[Crossref](#)], [[Google Scholar](#)], [[Publisher](#)]
- [23]. Yoo, D., Choi, M. S., Chung, C., Heo, S. C., & Choi, C., *J. Nanosci. Nanotechnol.*, 2013, **13**:7814 [[Crossref](#)], [[Google Scholar](#)], [[Publisher](#)]
- [24]. Xu X., Wang F., Li Z., Liu J., Ji J., Chen J., *Electrochim. Acta*, 2013, **87**:511 [[Crossref](#)], [[Google Scholar](#)], [[Publisher](#)]
- [25]. Hennayaka H., Lee H.S., *Thin Solid Films*, 2013, **548**:86 [[Crossref](#)], [[Google Scholar](#)], [[Publisher](#)]
- [26]. Zhou M., Liu D., Yu T., Cai Q., (2012, October). In 6th International Society for Optics and Photonics, 2012, **8419**:84192W [[Crossref](#)], [[Google Scholar](#)], [[Publisher](#)]
- [27]. Abdullah H., Habibi S., *Int. J. Photoenergy*, 2013, **2013** [[Crossref](#)], [[Google Scholar](#)], [[Publisher](#)]
- [28]. Ehsan M.A., Peiris T.N., Wijayantha K.U., Khaledi H., Ming H.N., Misran M., Mazhar M., *Thin Solid Films*, 2013, 540:1 [[Crossref](#)], [[Google Scholar](#)], [[Publisher](#)]
- [29]. Ramasamy K., Malik M.A., Helliwell M., Raftery J., O'Brien P., *Chem. Mater.*, 2011, **23**:1471 [[Crossref](#)], [[Google Scholar](#)], [[Publisher](#)]
- [30]. Agawane G.L., Shin S.W., Kim M.S., Suryawanshi M.P., Gurav K.V., Moholkar A.V., Kim J.H., *Curr. Appl. Phys.*, 2013, **13**:850 [[Crossref](#)], [[Google Scholar](#)], [[Publisher](#)]

- [31]. Bhaskar P.U., Babu G.S., Kumar Y.K., Jayasree Y., Raja V.S., *Mater. Chem. Phys.*, 2012, **134**:1106 [[Crossref](#)], [[Google Scholar](#)], [[Publisher](#)]
- [32]. Hastir A., Sharma S., Singh R.C., *App. Surf. Sci.*, 2016, **372**:57 [[Crossref](#)], [[Google Scholar](#)], [[Publisher](#)]
- [33]. Yuvaraj S., Fernandez A.C., Sundararajan M., Dash C.S., Sakthivel P., *Ceram. Int.*, 2020, **46**:391 [[Crossref](#)], [[Google Scholar](#)], [[Publisher](#)]
- [34]. Mariappan R., Ponnuswamy V., Bose A.C., Chithambararaj A., Suresh R., Ragavendar M., *Superlattices Microstruct.*, 2014, **65**:184 [[Crossref](#)], [[Google Scholar](#)], [[Publisher](#)]
- [35]. Ramachandran S., Dash C.S., Thamilselvan A., Kalpana S., Sundararajan M., *J. Nanosci. Nanotechnol.*, 2020, **20**:2382 [[Crossref](#)], [[Google Scholar](#)], [[Publisher](#)]
- [36]. Muhammed G.S., Abdullah M.M., Al-Sammarraie A.M.A., *Chem. Asian J.*, 2018, **30**:1374 [[PDF](#)], [[Google Scholar](#)]
- [37]. Tauc J., *Amorphous and liquid semiconductors*, Springer Science & Business Media, 2012 [[Google Scholar](#)], [[Publisher](#)]
- [38]. Suyver J.F., Wuister S.F., Kelly J.J., Meijerink, A., *Nano Lett.*, 2001, **1**:429 [[Crossref](#)], [[Google Scholar](#)], [[Publisher](#)]

HOW TO CITE THIS ARTICLE

Alaa Abd Al-Zahra, Abdul Karim M. A. Al-Sammarraie. Synthesis and Characterization of Zinc Sulfide Nanostructure by Sol Gel Method, *Chem. Methodol.*, 2022, 6(1) 67-73

DOI: 10.22034/chemm.2022.1.7

URL: http://www.chemmethod.com/article_139610.html